Plant Physiology and Biochemistry 139 (2019) 366–378

Contents lists available at ScienceDirect

Plant Physiology and Biochemistry

journal homepage: www.elsevier.com/locate/plaphy

Research article

Localization and expression analysis of a novel catalase from *Triticum monococcum* TmCAT1 involved in response to different environmental stresses

Sana Tounsi[a], Yosra Kamoun[b], Kaouthar Feki[a,c], Sonia Jemli[d], Mohamed Najib Saïdi[a], Hajer Ziadi[a], Carine Alcon[e], Faiçal Brini[a,*]

[a] Biotechnology and Plant Improvement Laboratory, Centre of Biotechnology of Sfax (CBS)/University of Sfax, B.P "1177", 3018, Sfax, Tunisia
[b] Laboratory of Molecular Biotechnology of Eukaryotes, Centre of Biotechnology of Sfax, B.P "1177", 3018, Sfax, Tunisia
[c] Laboratory of Legumes, Centre of Biotechnology Bordj Cedria, BP 901, 2050, Hammam Lif, Tunisia
[d] Laboratory of Microbial Biotechnology and Enzymes Engineering, Centre of Biotechnology of Sfax, B.P "1177", 3018, Sfax, Tunisia
[e] Biochimie & Physiologie Moléculaire des Plantes, PHIV Platform, UMR 5004 CNRS/386 INRA/Supagro Montpellier / Université Montpellier 2, Campus Supagro-INRA, 34060, Montpellier Cedex 2, France

ARTICLE INFO

Keywords:
Wheat
Catalase
Peroxisome
Peroxisomal targeting signal
Abiotic stress

ABSTRACT

Catalase proteins play a crucial role in detoxifying hydrogen peroxide, generated during plant growth, and in response to various environmental stresses. Despite their importance, little is known about their localization and expression in wheat. In this study, we identified and characterized a novel peroxisomal catalase gene from *Triticum monococcum*, designated as *TmCAT1*. Phylogenetic analysis revealed that TmCAT1 shared high identity with TdCAT1 and other plant catalases belonging to subfamily 1. We predicted the 3D structure model and the oligomerization arrangement of TmCAT1. Besides, we displayed an arrangement in asymmetric unit, which involved interactions including, mainly, residues from N-terminal domain. Interestingly, sequence analysis indicated that TmCAT1, like TdCAT1, had the peroxisomal targeting signal (PTS1) around its C-terminus. Transient expression of TmCAT1-GFP and TdCAT1-GFP in tobacco leaves revealed that the two fused proteins are targeted into peroxisomes. However, the truncated forms lacking the tripeptide QKL remained in the cytosol. Concerning the expression profile analysis, *TmCAT1* is expressed especially in leaves in normal condition. On the other hand, it is up-regulated by different stress incorporating salt, osmotic, oxidative, heavy metal and hormones stresses. Functional analysis by heterologous expression in yeast cells showed that *TmCAT1* improved tolerance to multiple abiotic stresses. The presence of important *cis*-regulatory elements in the promoter region of *TmCAT1* strongly reinforces the interest of this gene in plant adaptation to various stresses.

1. Introduction

Various abiotic stresses including drought, salinity and high temperature lead to the overproduction of reactive oxygen species (ROS) such as superoxide oxygen ($O2^{\bullet -}$), hydroxyl radical ($OH^{\bullet}$) and hydrogen peroxide (H_2O_2) in plant cells. These ROS are highly reactive and toxic and cause severe damage to proteins, lipids, and nucleic acid by imposing oxidative stress (Mittler, 2002; Miller et al., 2010; Scandalios, 2005; Choudhury et al., 2016). Under various stress conditions, ROS are mainly produced in different organelles like mitochondria, peroxisomes, chloroplast and probably other cellular compartments (Das et al., 2015). To avoid oxidative stress damage, plants possess very efficient scavenging systems incorporating enzymatic and non-enzymatic antioxidants (Choudhury et al., 2013; Noctor and Foyer, 2016; He et al., 2018). Among the enzymatic antioxidants, catalases are known as the most potential ROS scavengers owing to their high affinity for H_2O_2. In general, catalases are localized in peroxisomes and their activities are crucial for plants to remove excessive H_2O_2 by converting it to water and oxygen (Mhamdi et al., 2010; Su et al., 2014). Typical catalases, overall, have a peroxisomal targeting signal type 1 (PTS1) at the C-terminal part. The interaction between PTS1 and the receptor PEX5 in the cytosol is a key determinant for the entry of catalase into peroxisomes (Kamigaki et al., 2003; Oshima et al., 2008; Mhamdi et al., 2012). So far, various catalase genes have been identified in different plant species such as *Arabidopsis thaliana* (Frugoli et al., 1996), Zea mays (Guan and Scandalios, 1995),

* Corresponding author.
E-mail addresses: faical.brini@cbs.rnrt.tn, brinifaical2016@gmail.com (F. Brini).

https://doi.org/10.1016/j.plaphy.2019.03.039
Received 26 February 2019; Received in revised form 26 March 2019; Accepted 27 March 2019
Available online 30 March 2019
0981-9428/

rice (Iwamoto et al., 2000), barley (Skadsen, 1995) and wheat (Garcia et al., 2000; Feki et al., 2015). In *Arabidopsis*, catalase genes encode a small family of proteins including AtCAT1, AtCAT2, and AtCAT3. Two genes are located closely on chromosome 1 (*AtCAT1* and *AtCAT3*) and one is found on chromosome 4 (*AtCAT2*) (Frugoli et al., 1996; Mhamdi et al., 2012). The transcription level of *Arabidopsis* catalases is regulated both temporally and spatially and responds differentially during developmental process and in response to various environmental factors (Zimmermann et al., 2006; Du et al., 2008). It was reported that *AtCAT1* is expressed in leaves; *AtCAT2* is expressed in photosynthetic tissues, whereas *AtCAT3* expression is important in vascular tissues and senescent leaves (Zimmermann et al., 2006; Du et al., 2008; Mhamdi et al., 2012). The involvement of catalase genes in both abiotic and biotic stress responses has been demonstrated in numerous studies (Giri et al., 2017; Su et al., 2018). Recently, it has reported that the deletion of all *Arabidopsis* catalases (*cat1/2/3*) causes a negative effect on plant growth, catalase activity, redox state and a strong sensitivity to abiotic stresses, suggesting that catalases play a central role in scavenging H_2O_2 at different developmental stages and in response to diverse environmental stresses (Zimmermann et al., 2006; Du et al., 2008; Mhamdi et al., 2012; Su et al., 2018). In rice, three catalase genes *OsCATA*, *OsCATB*, and *OsCATC* were identified and expressed in the leaf sheath, root and leaf blade, respectively (Iwamoto et al., 2000). Moreover, they were up-regulated in response to various abiotic and biotic stresses (Alam and Ghosh, 2017). So far, only two catalase isoforms have been isolated from bread wheat (*Triticum aestivum*, AABBDD) and only one gene has been characterized from durum wheat (*Triticum durum*, AABB) (Garcia et al., 2000; Feki et al., 2015). Transgenic rice plant overexpressing bread wheat catalase showed enhanced tolerance only to cold stress (Matsumura et al., 2002). In contrast, the expression of *TdCAT1* in *Arabidopsis* plants conferred tolerance to various abiotic stresses (Feki et al., 2015). To our knowledge, no catalase gene in the diploid wheat ancestor (*Triticum monococcum*, AA) has been identified. Thus, in this study, we isolated the full-length *TmCAT1* cDNA sequence from *T. monococcum*, which is homologous to durum wheat gene *TdCAT1*. We determined its functional domains, genomic organization, sequence homology with other catalases and the three-dimensional structure. Moreover, we evaluated the expression pattern and the role of *TmCAT1* of yeast cells in response to various environmental stresses. These results provide new insight into the understanding of the physiological functions of catalase genes in wheat.

2. Materials and methods

2.1. Plant material and stress treatments

Seeds of *T. monococcum* (cv. Turkey) were provided by the ICARDA (Genetic resources Unit, Syria). They were treated with 10% potassium hypochlorite solution for 15 min, thoroughly washed three times with sterile water and germinated on a sheet of Whatman filter paper placed in a Petri dish. The dishes were stored in a growth room at 23 °C and 65% relative humidity, under light/dark conditions of 16 h light at 250 μmol m^{-2} s^{-1}/8 h dark.

For quantitative real-time PCR analysis, seven days after germination on filter paper moistened with sterile water, the seedlings were transferred to hydroponic culture conditions onto half-strength Hoagland solution (Davenport et al., 2005). After 15 days, stress treatments were applied. The seedlings were transferred to different solutions, containing 100 mM NaCl, 10 mM H_2O_2, 15% PEG (w/v), 100 μM ABA, 5 mM salicylic acid (SA) and 100 μM $CdCl_2$. Control seedlings were kept in half-strength Hoagland medium. Plant tissue samples (roots and leaves) were collected after 24 and 72 h of stress treatments, immediately frozen in liquid nitrogen and stored at −80 °C until RNA extraction and expression analyses.

Table 1
List of primers used in this study. The underlined sequences correspond to *Eco*RI restriction enzyme.

Primer	Sequence (5′-3′)	Strategy
TmCAT1-F	CTGAATTCATGGACCCCTACAAGTAC	RT-PCR
TmCAT1-R	CTGAATTCTTACATGCTCGGCTTGGA	
qTmCAT1-F	CGAGAAGATGGTGATCGAGAA	Q-PCR
qTmCAT1-R	TGTTGATGAATCGCTCTTGC	
qAct-F	TGCATAGAGGGAAAGCACG	
qAct-R	AACCCAAAAGCCAACAGAGA-	
gCAT1-F	CACCATGGACCCCTACAAGTACCG	Subcellular localization vector construction
gCAT1-R	CATGCTCGGCTTGGAGCTG	
gCAT1-R-PTS	GCCGAGAGACTTGTCAGCCTGAGACC	
TmCAT1-G1	TGATGGCGAAGCCGCGCGGGTC	Isolation of *TmCAT1* promoter
TmCAT1-G2	GTCAGGTGGGAGACGTCGTGGGT	
TmCAT1-G3	CGACGGTGAGGGAGTTGTCGTTG	
TmCAT1-G4	GGCCGGTACTTGTAGGGGTCCAT	
R1	NGTCGASWGANAWGAA	
R2	GTNCGASWCANAWGTT	
R3	WGTGNAGWANCANAGA	
R4	NCAG CTW SCTNTSCTT	

2.2. Isolation and molecular cloning of TmCAT1 cDNA

Total RNA were isolated from *T. monococcum* plants subjected to 100 mM NaCl during 2 days, using the Trizol reagent (Invitrogen) according to the manufacturer's protocol. Then, RNA was treated with RNase-free DNase to remove the remaining genomic DNA. First-strand cDNA was synthesized from 2 μg of total RNA, using M-MLV reverse transcriptase (Invitrogen), according to the manufacturer's protocol. The cDNA of *TmCAT1* was amplified using a couple of specific primers TmCAT1-F and TmCAT1-R derived from *TdCAT1* sequence (accession no. KP696753) (Table 1). The primers TmCAT1-F and oligo-dT were used to verify the 3′ region, whereas the 5′ region was identified using the HE-TAIL-PCR method as described below. The PCR protocol consisted of an initial denaturation at 94 °C for 5 min followed by 35 cycles comprising a first step at 94 °C for 30 s, an annealing step at 55 °C for 30 s and elongation at 72 °C for 1 min, and a final 10 min extension at 72 °C. PCR products were gel-purified, cloned in the pGEM-T Easy vector and sequenced using T7 and SP6 primers.

2.3. Real-time quantitative PCR analysis

The expression profile of *TmCAT1* was determined using quantitative expression analysis. Primers were designed with Primer 3 software for *TmCAT1* and *actin* genes using the following gene-specific primers: *TmCAT1* (qTmCAT1-F, qTmCAT1-R) and *actin* (qACT-F, qACT-R) (Table 1). Real-time PCR was performed in 96-well plates with the CFX 96 Touch TM Real-Time PCR System (Biorad) using SYBR @ Select Master Mix for CFX (Applied Biosystems). The amplification reactions were performed in 10 μl final volumes containing 5 μl 2 × SYBR @ Select Master Mix, 0.5 μl of each primer (10 μM), 1 μl of RNase-free water and 3 μl DNA (40 ng of cDNA). The reaction consisted of an initial denaturation at 94 °C for 10 min, followed by 45 cycles at 94 °C for 10 s, 60 °C for 10 s and 72 °C for 15 s, then a melting curve (5 s at 95 °C, 1 min at 65 °C and 5 min with temperature increasing from 65 to 97 °C). The relative expression was quantified using the comparative CT method with the *actin* gene as an internal expression standard (Livak and Schmittgen, 2001). The relative expression was determined using formula $2^{-\Delta\Delta CT}$. Three biological repetitions were performed for each experimental condition, with three technical repetitions for each sample.

2.4. Bioinformatics analysis

Multiple sequence alignments of catalase protein sequences from *T. monococcum* and other species were performed using Clustal W software

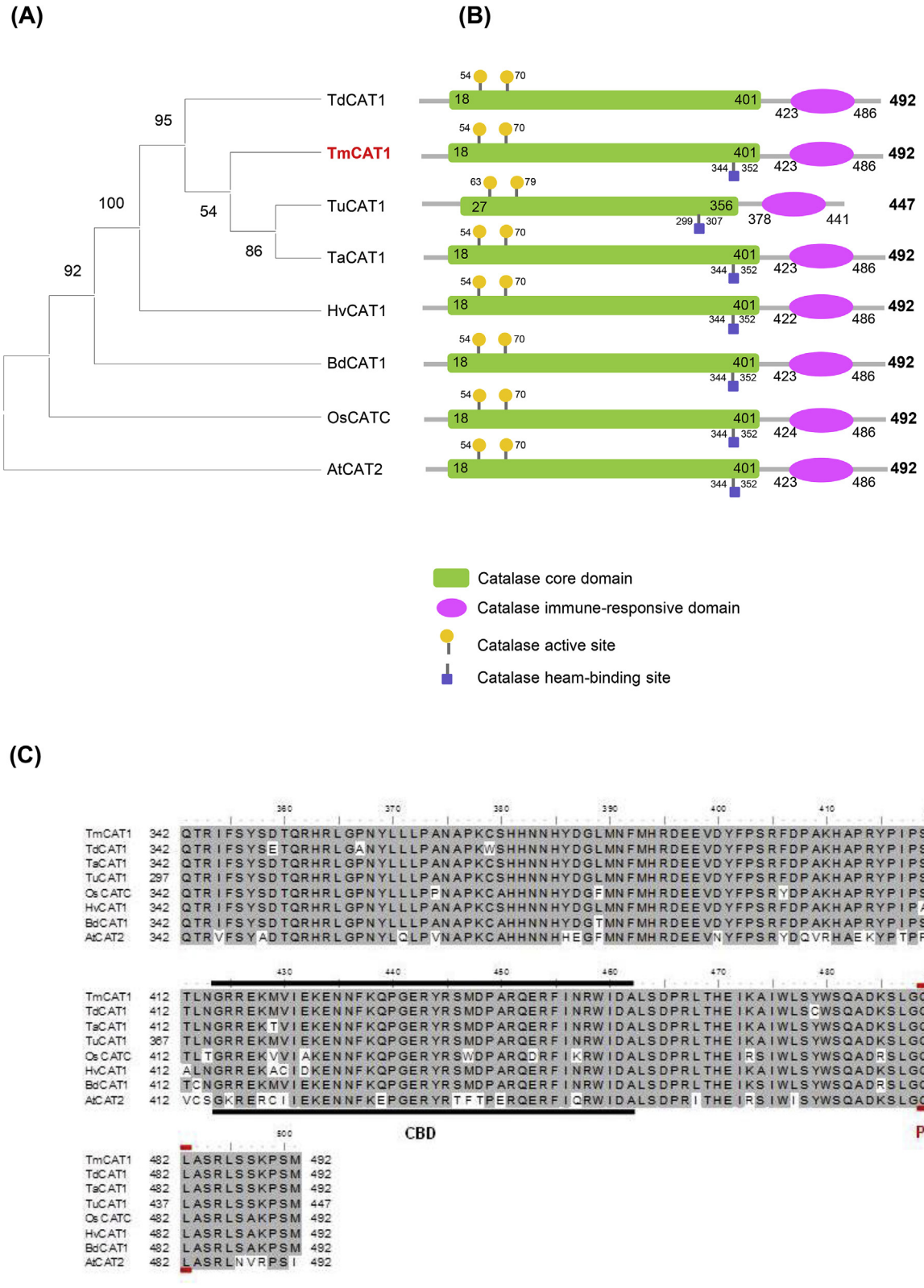

Fig. 1. Phylogenetic analysis, functional domains and protein sequence alignment of TmCAT1 with other plant catalases. (A) The phylogenetic tree was constructed using the Neighbor-Joining method with 1000 bootstrap replicates, based on amino acid sequences from phytozome, gramene and NCBI databases. The protein accession numbers are: *Triticum turgidum* TdCAT1 (KP696753), *Triticum aestivum* TaCAT1 (TRIAE_CS42_5AL_TGACv1_376544_AA1238210), *Triticum urartu* TuCAT1 (TRIUR3_26493), *Hordeum vulgare* HvCAT1 (HORVU4Hr1G082040), *Brachypodium distachyon* BdCAT1 (BRADI1G76330), *Oryza sativa* OsCATC (LOC_Os03g03910), *Arabidopsis thaliana* AtCAT2 (AT4G35090). (B) Functional domains analysis of CAT1 protein sequences using InterPro tool. (C) Protein sequence alignment of TmCAT1 with other plant catalase proteins. The putative calmodulin binding domain (CBD) and putative peroxisomal targeting signal (PTS1) binding domain are overlined.

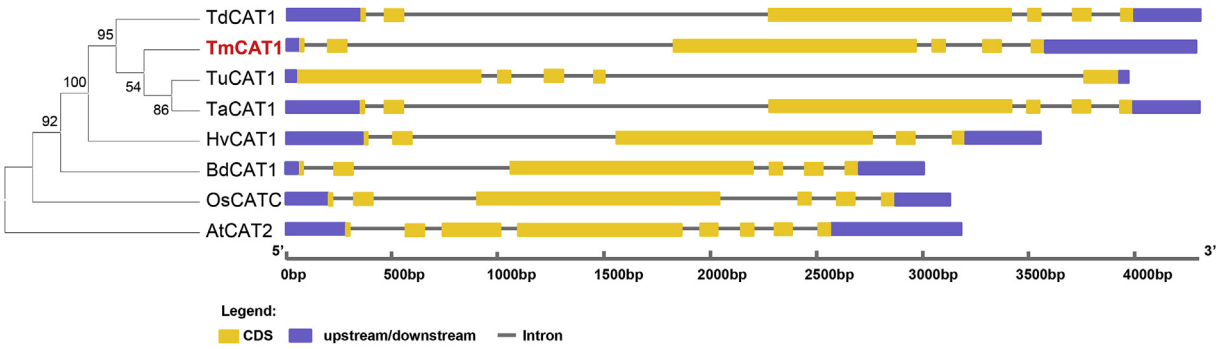

Fig. 2. Gene structure analysis of *TmCAT1* and other catalase genes from wheat, barley, *Brachypodium*, rice and *Arabidopsis* using GSDS tool.

(http://www.clustal.org/). The phylogenetic tree was carried out using the Neighbor-joining method based on the number of amino acid substitutions per site and the bootstrap test with 1000 replicates. Ka/Ks calculation was performed by means of MEGA 6.06 and the Nei-Gojobori method. The gene structure was identified using Gene Structure Display Server (GSDS, http://gsds.cbi.pku.edu.cn). The ProtParam online tool (http://web.expasy.org/protparam/) was used to determine the physico-chemical parameters of TmCAT1. The InterPro tool available on the EBI web page (http://www.ebi.ac.uk/interpro/) was used to identify the functional domains from the TmCAT1 sequence. The presence of putative stress-responsive *cis*-regulatory elements on the promoter region of catalase genes were performed using PlantCARE database (http://bioin forma tics.psb.ugent.be/webto ols/plant care/htmlU H).

2.5. Molecular modeling and structural analysis

The automated protein structure homology modeling server, Swiss Model (http://www.expasy.org/swissmod/), was used to generate the three-dimensional model of TmCAT1. Generated models were further refined by two-step atomic-level energy minimization through the ModRefiner tool (http://zhanglab.ccmb.med.umich.edu/ModRefiner/). Then, the models were evaluated and validated by Ramachandran plots created by the online tool RAMPAGE (http://mordred.bioc.cam.ac. uk/~rapper/rampage.php). The monomeric models were, afterwards, served for the generation of the tetrameric structure using the SymmDock docking server (http://bioinfo3d.cs.tau.ac.il/SymmDock/). SymmDock is an algorithm for the prediction of complexes with Cn symmetry by geometry based docking (Schneidman-Duhovny et al., 2005). Given the structure of the asymmetric unit of the multimer complex, SymmDock predicts the structure of the entire complex. A Cn symmetry type complex is a complex with a rotational symmetry of order n about a symmetry axis. The rotation angle alpha is of 360/n degrees. For this study, n was set to 4 and the default parameters of SymmDock were input. The RING 2.0 web server (available at: http://protein.bio.unipd.it/ring) was used for visualizing the interactions at an atomic level in the quaternary structure (Piovesan et al., 2016). The RING 2.0 output file was then evaluated using the online tool PDBePISA (http://www.ebi.ac.uk/pdbe/pisa/) to identify the amino acid residues involved in interchain hydrogen bonds and salt bridges. The PyMOL v0.99 program (http://www.pymol.org) was used to visualize and analyze the generated model structure and to construct graphical presentations and illustrative figures.

2.6. Subcellular localization of wheat CAT1 proteins

To determine the subcellular localization of TmCAT1 and TdCAT1 (Feki et al., 2015), the coding region of both genes was amplified using the primers gCAT1-F and gCAT1- R (Table 1). To delete the 13 amino acids at the C-terminal part of these two proteins, TmCAT1 and TdCAT1 were re-amplified using the primers gCAT1-F and gCAT1-R-PTS (Table 1) to obtain the two truncated forms TmCAT1Δ_{PTS1} and TdCAT1Δ_{PTS1}, without PTS1 domain. The gateway cloning was carried out to have a C-terminal protein fusion with GFP. The four constructs, pENTR-TmCAT1, pENTR-TmCAT1Δ_{PTS1}, pENTR-TdCAT1 and pENTR-TdCAT1Δ_{PTS1}, were recombined into the destination vector, pB7FWG2 using LR clonase (Invitrogen). The recombinant plasmids were verified by PCR and the sequencing was followed by the transfection of the cells of *Agrobacterium tumefaciens* strain GV3101 by the freeze-thaw method (Weigel and Glazebrook, 2006).

The TmCAT1:GFP, TmCAT1Δ_{PTS1}:GFP, TdCAT1:GFP and TdCAT1Δ_{PTS1}:GFP fusion constructs were transiently co-expressed in tobacco leaf epidermal cells with the plasmid px-rk CD3-983 coding for a peroxisomal marker (Nelson et al., 2007). *Nicotiana tabacum* leaves were agro-infiltrated with the recombinant *Agrobacterium tumefaciens* strains (strain GV3101, infiltration solution OD_{600} = 0.1) according to Sparkes et al. (2006). After two days, confocal imaging was performed using a Leica TCS SP8 laser scanning microscope with a 40X oil N.A. 1.1 immersion objective. Emission fluorescence of GFP and mCherry was collected by line sequential scanning mode at 488 nm and 561 nm excitation, respectively. The emitted signal was collected between 500-535 and 590–620 for GFP and mCherry, respectively. Images were processed using ImageJ software.

2.7. Expression of TmCAT1 in yeast

The wild-type *S. cerevisiae* strain used in this study was W303.1A (*MATa ade2 ura3 leu2 his3 trp1*). The open reading frame (ORF) of *TmCAT1* gene was digested from pGEM-T Easy-*TmCAT1* using the *Eco*RI restriction enzyme, gel-purified and inserted into the *Eco*RI site of the yeast expression vector pYES2 vector. After checking the orientation of the *TmCAT1* cDNA relative to the GAL promoter, the resulting plasmid pYES2-*TmCAT1* and the empty pYES2 were then introduced into *Saccharomyces cerevisiae* cells using the PEG lithium acetate transformation method (Gietz et al., 1995). The recombinant yeast clones selected on yeast nitrogen base plates lacking uracil (YNBUra$^-$) were verified by PCR.

To determine the role of TmCAT1 protein in yeast, stress tolerance assays were performed using the YNBUra$^-$+ Galactose 2% solid medium, containing or not 0.5 M NaCl, 4 μM H_2O_2, 1.2 M mannitol and 0.1 M LiCl. To test the heat stress tolerance, yeast cells were placed in water bath at 48 °C for 6 h. Aliquots from saturated yeast cultures (5 μl) and tenfold serial dilutions (10^{-1}, 10^{-2} and 10^{-3}) were spotted onto these media and incubated at 30 °C for 5 days. Aliquots from saturated yeast liquid cultures were counted and adjusted to 10^7 cells/ml, as an initial cell concentration. Then, a serial dilution with ten-fold dilution factor was prepared (10^{-1}, 10^{-2} and 10^{-3}) and spotted on (5 μl) per drop onto solid medium (YNB-Glu and YNB-Gal), then incubated at 30 °C for 5 days. The percentage of viable cells after different treatments was calculated as follows: (number of colonies in YNB-Gal/number of colonies in YNB-Glu) × 100.

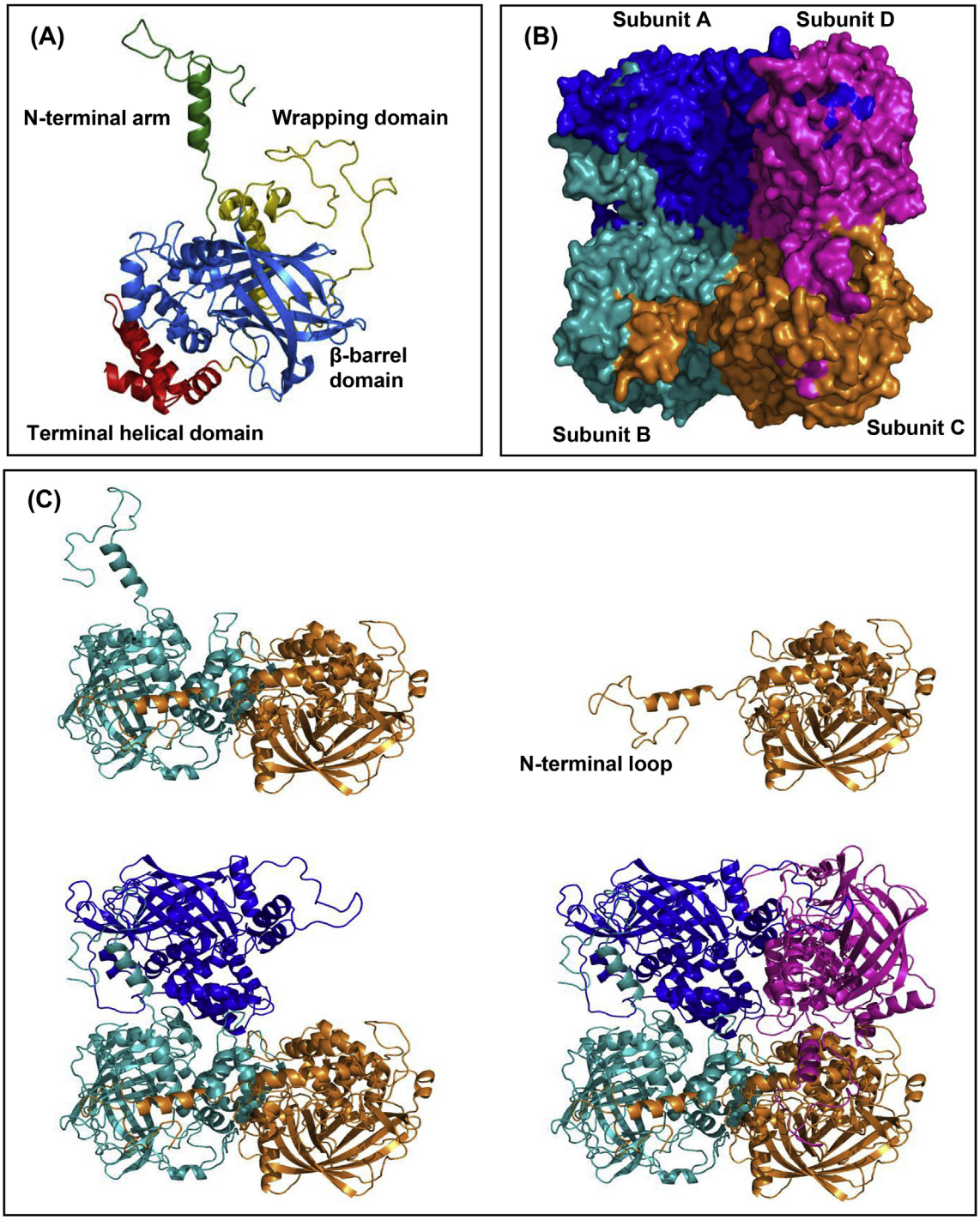

Fig. 3. Prediction of three-dimensional structure of TmCAT1. (A) Ribbon structure of a monomer of TmCAT1, showing the four distinct structural regions: the N-terminal arm (green), the β-barrel domain (blue), the wrapping domain (yellow) and the α-helical domain (red). (B) Surface representation of the TmCAT1, tetrameric structure predicted by SymmDock server; subunits A (blue), B (cyan), C (orange) and D (magenta). (C) Ribbon representation of TmCAT1, showing the predominant involvement of the N-terminal domain in subunits oligomerization. (For interpretation of the references to colour in this figure legend, the reader is referred to the Web version of this article.)

2.8. Isolation and cloning of TmCAT1 promoter by HE-TAIL-PCR method

To isolate the 5′-flanking region of *TmCAT1*, the high-efficiency thermal asymmetric interlaced (HE-TAIL) PCR method was performed (Michiels et al., 2003). PCR reactions were carried out with genomic DNA, extracted from *T. monococcum* leaves, as template, four gene-specific reverse primers (TmCAT1-G1; TmCAT1-G2; TmCAT1-G3 and TmCAT1-G4) (Table 1) designed close to the *TmCAT1* 5′UTR sequence, and four arbitrary degenerate primers (Rn1, Rn2, Rn3 and Rn4) (Table 1). Three rounds of PCR were performed using the product of the previous PCR, as template, for the next PCR. To determine appropriate product lengths, products of the tertiary PCR, with the control (Rn–Rn), were loaded on a 1% agarose gel. Target bands, identified using the couple of primers TmCAT1-G3/R3 and TmCAT1-G4/R3, were ligated into the pGEM-T Easy. A total promoter "*PrTmCAT1*" sequence about 900 bp was obtained by the sequencing of four positive clones using T7

Table 2
Residues Interaction bonds involved in the oligomerization between two neighboring subunits of TmCAT1 tetramer.

N°	Subunit A	Distance (Å)	Subunit D
Hydrogen bonds			
1	Leu32 [O]	2.78	Asn374 [ND2]
2	Ser36 [OG]	3.31	Cys370 [SG]
3	Pro39 [O]	3.38	Asn374 [ND2]
4	Ile40 [O]	2.35	His372 [NE2]
5	Glu43 [O]	2.28	Asn375 [H]
6	Glu57 [OE2]	3.49	Arg417 [NH1]
7	Asn161 [O]	3.66	Arg171 [NH2]
8	Gly245 [O]	2.11	Asn427 [ND2]
9	Ala246 [O]	2.28	Asn427 [ND2]
10	Ile312 [O]	3.20	Arg416 [NH2]
11	Ser36 [OG]	3.25	Arg129 [O]
12	Gln167 [H]	2.48	Asp174 [OD1]
13	Gly38 [H]	2.08	Ser371 [O]
14	Asn30 [ND2]	3.81	Ala403 [O]
15	Asn27 [ND2]	3.68	Ala403 [O]
16	Asn30 [ND2]	2.82	Tyr406 [O]
17	Phe315 [H]	1.72	Arg417 [O]
18	Arg67 [NH1]	3.70	Lys419 [O]
19	Asn169 [ND2]	3.87	Glu462 [OE1]
20	Arg117 [NH1]	2.51	Glu462 [OE2]
Salt bridges			
1	Glu57 [OE2]	3.49	Arg417 [NH1]
2	His248 [NE2]	3.17	Glu181 [OE1]
3	Arg117 [NH1]	3.18	Glu462 [OE1]
4	Arg117 [NE]	4.00	Glu462 [OE2]
5	Arg117 [NH1]	2.51	Glu462 [OE2]
6	Arg117 [NH2]	3.79	Glu462 [OE2]

and SP6 primers.

2.9. Statistical analysis

Each experiment was repeated thrice; the mean values and standard deviation were calculated. A one-way analysis of variance (ANOVA) was performed followed by an appropriate Duncan post hoc test using the SPSS ver.13 statistical package. Values were calculated at $P \leq 0.001$ to determine the significance of difference between the means. Mean values that were significantly different were indicated by different alphabets.

3. Results

3.1. Isolation and sequence analysis of TmCAT1

The coding region of catalase gene *TmCAT1* was amplified by RT–PCR using as template the total RNA extracted from *T. monococcum* exposed to 100 mM NaCl for 2 days. After sequencing, the analysis of the primary sequence revealed that the open reading frame (ORF) of *TmCAT1* is 1479 bp and it encoded to a protein of 492 amino acids with a predicted molecular weight (MW) of 56 KDa and a calculated isoelectric point (PI) of 6.65. The *TmCAT1* sequence was deposited into GenBank with the accession number (MK091459).

The amino acids sequence comparison revealed that TmCAT1 exhibited high sequence identity with TdCAT1 from *T. durum* (98% of identity). To investigate the phylogenetic relationship of TmCAT1 with other plant catalase proteins, a phylogenetic tree was constructed using MEGA 6 program. As illustrated in Fig. 1A, TmCAT1 was closely related to catalase proteins from durum (TdCAT1) and bread wheat (TaCAT1), *T. urartu* (TuCAT1), and *H. vulgare* (HvCAT1), which belong to class I. Furthermore, the putative functional domains of TmCAT1 were identified using the InterPro tool, which are the catalase core domain (also designed IPR011614) and the catalase immune-responsive domain (also designed IPR010582) from residues 18 to 401 and from 423 to 486, respectively. The potential active sites of this protein are located from residues positions 54 to 70, whereas the catalase heme binding sites are expected to be situated from residues 344 to 352 (Fig. 1B). Structure analysis revealed that all these domains are present in wheat, barley, rice, *Brachypodium* and *Arabidopsis* CAT1 proteins, except TdCAT1. Thus, we suggested that the domain structure for catalase proteins was highly conserved in different species.

Moreover, TmCAT1 protein has the PTS1 motif (QKL), in the residues positions Q480 to L482, like other peroxisomal CAT proteins (Fig. 1C). It has been reported that this conserved motif interacts directly with PTS1 receptor protein Pex5p allowing the entry of catalases into peroxisomes (Kamigaki et al., 2003; Wang et al., 2017). On the other hand, TmCAT1 presents a putative calmodulin binding domain (CBD), located at the residue G415 to I451 (Fig. 1C). The presence of this domain was found in various CAT1 proteins, namely SPCAT1 (Chen et al., 2012) and TdCAT1 (Feki et al., 2015). The CBD domain plays an important role in calmodulin binding and the activation of some plant catalases in the presence of calcium (Yang and Poovaiah, 2002).

The analysis of exon-intron organizations of *TmCAT1* with other *CAT* genes showed high conservation of exon length and intron number between *TmCAT1*, *TdCAT1* and *TaCAT1* genes (Fig. 2). *AtCAT*2 has the largest number of exons (7), however, *TuCAT*1 and *HvCAT1* have the lowest number of exons (5). Although the size of the catalase genes varied from 3 kb in *Arabidopsis* to 4.5 kb in *TmCAT1*, *TdCAT1* and *TaCAT1*, the encoded proteins contained the same number of amino acids.

Overall, we suggested that TmCAT1 belongs to the monofunctional heme-containing catalases types, is a putative peroxisomal catalase protein, and it is potentially regulated and activated by calmodulin and calcium.

3.2. Prediction of the three-dimensional structure of TmCAT1

To determine the three-dimensional structure of TmCAT1, we used the crystal structure of the catalase of *Bacillus pumilus* (pdb code: 4QOL) as a template (Loewen et al., 2015). This analysis showed the presence of four distinct regions typical of monofunctional catalases, which are the N-terminal arm (to Val64), the conserved anti-parallel eight-stranded β-barrel (His65 to Ile312), the extended wrapping loop (Asp313 to Asn426) and the C-terminal helical domain (Asn427 to Met492) (Fig. 3A). A part of the β-barrel domain and wrapping domain forms the heme pocket, which is composed by five essential residues: His65, Serl04, Asn138, Arg344 and Tyr348. As described by Chen et al. (2012), the three amino acids His, Ser and Asn form the conserved catalytic residues.

As catalases are typically formed by four identical subunits, the homotetramer structure of TmCAT1 was generated by the docking server SymmDock. The structure examination revealed that the four protein chains oligomerized in an asymmetric unit form, in which subunit A is connected to subunit D and this latter is connected to subunit C. The latter subunit is consecutively connected to subunit B which is reconnected to subunit A (Fig. 3B and C). As shown in Fig. 3C, the N-terminus domain or arm domain of each subunit is notably involved into contact with neighboring chain, making subunits association deeply interconnected. The careful examination of the contact surface connecting two adjacent subunits of TmCAT1 in the predicted 4D-arrangement displayed twenty hydrogen bonds and six salt bridge interactions, suggesting a close oligomerization (Table 2). In this arrangement, the N-terminal domain contributed to the establishment of 55% of hydrogen bounds, while the C-terminal domain is responsible for the establishment of about 66% of salt bridges. The finding is in accordance with other studies, suggesting that oligomerization arrangement largely involved N or C terminus interactions by contact polar neighboring subunits interface (Caffery et al., 2004).

3.3. Determination of wheat CAT1 subcellular localization

So far, the subcellular localization of wheat catalases has not yet

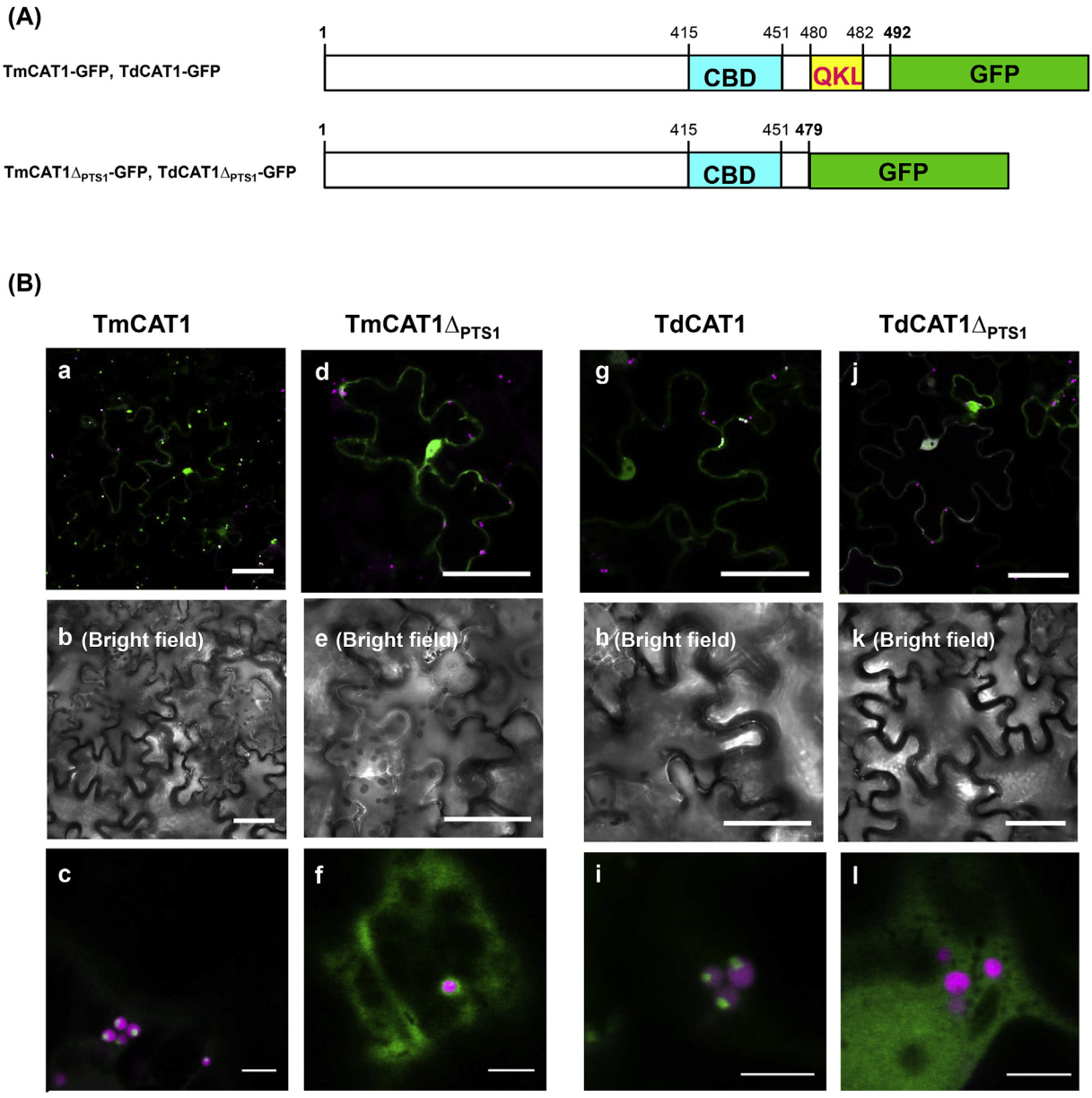

Fig. 4. Driving of TmCAT1 and TdCAT1 to the peroxisomes by PTS1 system in tobacco cells. (A) Schematic representation of TmCAT1 and TdCAT1 fragments fused in frame with GFP. The putative calmodulin binding domain (CBD) and the putative peroxisomal targeting signal (PTS1) positions are indicated. (B) Confocal microscopy observations of the wild-type and truncated constructs of TmCAT1 and TdCAT1 fusion proteins in agro-infiltrated tobacco leaf. Co-expression of TmCAT1-GFP (a, b, c), TmCAT1Δ_{PTS1}-GFP (d, e, f), TdCAT1-GFP (g, h, i) and TdCAT1Δ_{PTS1}-GFP (j, k, l) with the peroxisomal marker construct Px-rk983-mcherry. Fluorescence of GFP (green) and mcherry (magenta) were monitored 48 h after the leaf infiltration. Bars: (a, b, f, g, k, l) 50 µm; (c, d, e, h, i, j) 5 µm. (For interpretation of the references to colour in this figure legend, the reader is referred to the Web version of this article.)

been characterized. Recently, Feki et al. (2015) have identified the first durum wheat catalase TdCAT1, which contains a putative consensus internal PTS1 motif potentially involved in peroxisomal targeting. Like TdCAT1, TmCAT1 has an internal PTS1, composed of three essential amino acids (QKL) in the C-terminal part. In order to determine the role of the conserved peroxisomal targeting signal of the two catalases TmCAT1 and TdCAT1, we deleted the 13 amino acids at the end of these two proteins, and the two truncated forms were fused to GFP under the control of the promoter 35S. Then, the constructs with the two deleted forms (p35S:TmCAT1Δ_{PTS1}-GFP and p35S:TdCAT1Δ_{PTS1}-GFP) and with the two whole proteins (p35S:TmCAT1-GFP and p35S:TdCAT1-GFP) were co-transformed with the peroxisomal marker construct Px-rk983-mcherry into tobacco leaf cells (Fig. 4A). Confocal microscopy analyses indicated that TmCAT1-GFP and TdCAT1-GFP fusion proteins were strongly accumulated in the peroxisomes and faintly in cytoplasm (Fig. 4B, c and i). By contrast, when the tripeptide QKL was deleted, the GFP signal of the TmCAT1Δ_{PTS1}-GFP and TdCAT1Δ_{PTS1}-GFP was not detected in the peroxisomes (Fig. 4B, f and l). Taken together, we suggested that PTS1 motif is essential for the peroxisomal localization of these two wheat CAT proteins.

3.4. qRT-PCR analysis of TmCAT1 gene expression

Tissue-specific expression of *TmCAT1* was investigated using real-time RT-PCR in different tissues of *Triticum monococcum.* Moreover, the level of transcriptional expression under various abiotic stresses was analyzed. Under control condition, *TmCAT1* gene was significantly expressed in the photosynthetic part especially in leaves; however, this expression was very low in roots (Fig. 5). Thus, we suggested that *TmCAT1* gene may play a crucial role in the scavenging of H_2O_2

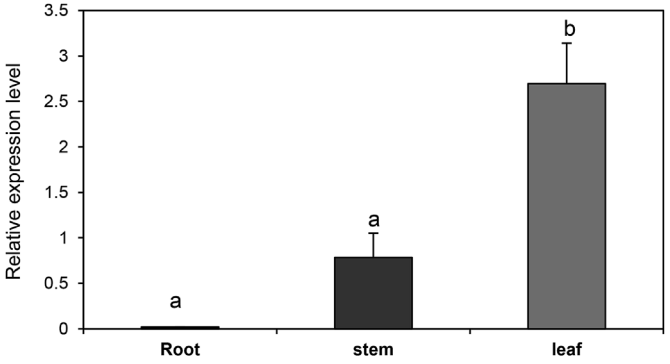

Fig. 5. Real-time RT–PCR analysis of *TmCAT1* expression in different tissues of *Triticum monococcum* grown under standard condition. Data are normalized to the *actin* expression level. Data are means ± SE of three biological replicates.

generated during plant growth.

To gain insight into the involvement of *TmCAT1* in response to various stress conditions, we analyzed its expression in roots and leaves under salt (100 mM NaCl), oxidative (10 mM H_2O_2), osmotic (15% PEG), abscisic acid (100 µM ABA), salicylic acid (5 mM SA) and heavy metal (100 µM $CdCl_2$) stresses for 24 h and 72 h. As indicated in Fig. 6, the expression of *TmCAT1* is strongly induced in roots and reached its maximum accumulation after 48 h of salt and oxidative stresses and 72 h of heavy metal treatment. On the other hand, under osmotic stress, *TmCAT1* was around 7 fold induced in roots at 24 h stress, compared to control condition (Fig. 6). The treatment with 100 µM ABA and 5 mM SA had little effect on *TmCAT1* expression in roots. By contrast, in leaves, the transcript level of *TmCAT1* was increased by a factor close to 3 and 4 after 3 days of abscisic acid and salicylic acid treatments, respectively (Fig. 6). These findings suggest that *TmCAT1* could be a positive responsive component of abiotic stress in *Triticum monococcum* plant.

3.5. Overexpression of TmCAT1 in yeast cells improves tolerance to abiotic stresses

The biological role of *TmCAT1* in abiotic stress tolerance was investigated by heterologous expression in yeast cells. The full-length cDNA was cloned in the pYES2 yeast expression vector under the control of the constitutive expression promoter GAL1 and transformed into *S. cerevisiae* strain. Yeast strains expressing *TmCAT1* and the control strains transformed with the empty vector (pYES2) grew equivalently under normal condition (Fig. 7A). However, in the presence of NaCl, H_2O_2, mannitol and heat stresses, the cells expressing *TmCAT1* exhibited a better growth compared to the control cells (Fig. 7A). The number of the recombinant cells was about 1.5 fold higher than control cells under NaCl, mannitol and heat stresses. On the other hand, in the presence of LiCl in the medium, the growth rate of the yeast cells expressing *TmCAT1* was similar to the control yeast cells (Fig. 7B). It is noteworthy that the growth of yeast cells, expressing *TmCAT1* under direct oxidative stress, was enhanced eight times more than the strain transformed with the empty vector. These results indicated that the expression of *TmCAT1* in yeast cells improved their growth under different stress conditions.

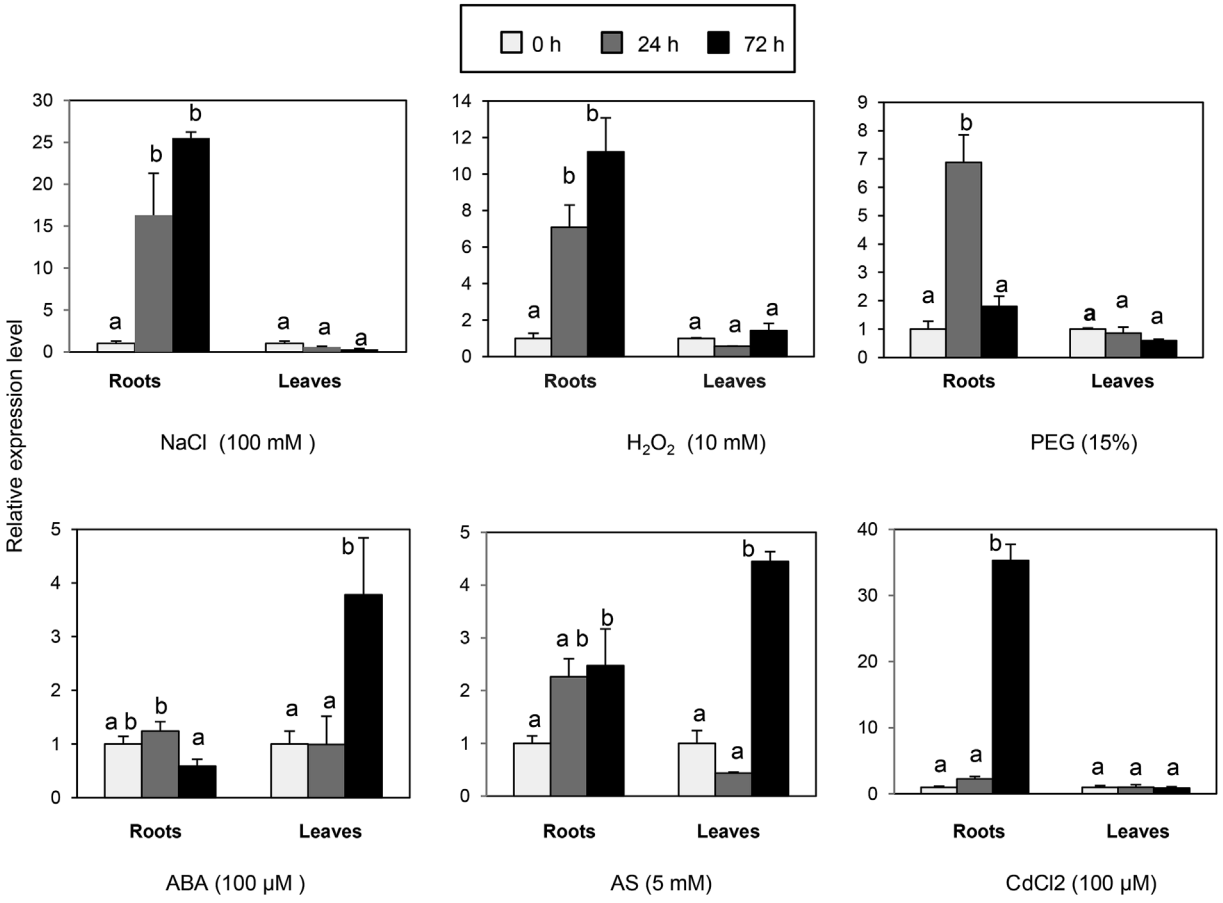

Fig. 6. Variation of *TmCAT1* transcript accumulation in roots and leaves of *Triticum monococcum* plants in response to different environmental and hormonal treatments. The expression level of *TmCAT1* was analyzed after the addition of 100 mM NaCl, 10 mM H_2O_2, polyethylene glycol (PEG) 15%, 100 µM ABA, 5 mM salicylic acid and 100 µM $CdCl_2$ for 24 and 72 h. Transcript levels are given relative to the average levels in control plants (kept in standard conditions), at the same time. Data are means ± SE of three biological replicates.

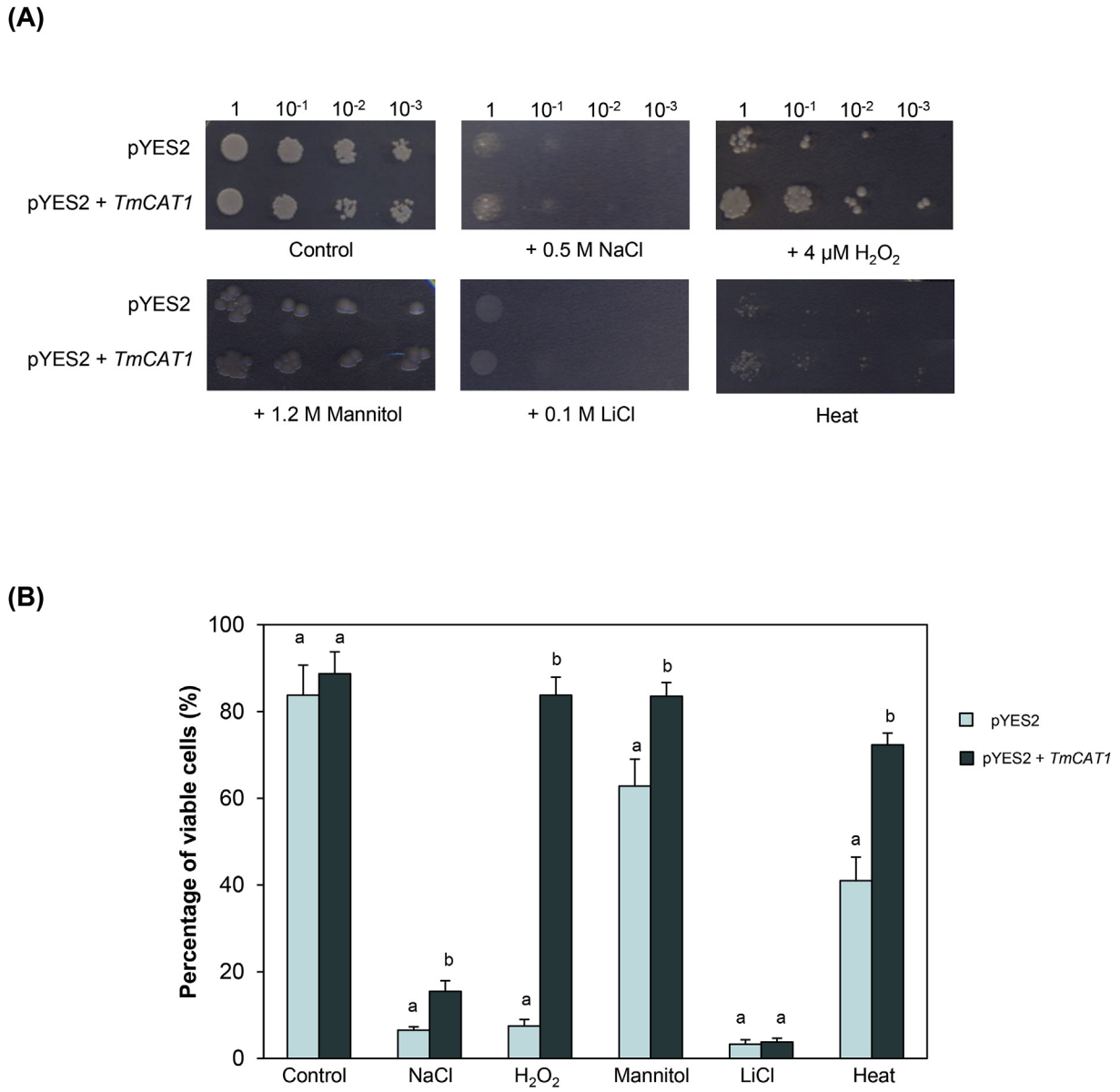

Fig. 7. Functional characterization of *TmCAT1* expressed in *S. cerevisiae* in response to abiotic stress. (A) Yeast cells transformed with the empty vector (pYES2) and with the recombinant vector (pYES2 + *TmCAT1*) were grown for 5 days under normal growth conditions (YNB-Ura/Gal2%) or after the addition of 0.5 M NaCl, 4 µM H_2O_2, 1.2 M mannitol, 0.1 M LiCl and under heat (48 °C). (B) Presentation of percentage of viable cells under control, salt, oxidative, osmotic, ionic and heat conditions. Data presented are means of at least 3 independent experiments ± S.E. Bars carrying diverse letters are significantly different ($p \leq 0.001$) from each other, according to Duncan test results, while bars carrying the same letters are not significantly different.

3.6. Isolation and in silico analysis of TmCAT1 promoter

To further understand the regulatory mechanism of *TmCAT1* gene expression, the promoter region of *TmCAT1* was isolated using the thermal asymmetric interlaced PCR (TAIL-PCR) technique. As illustrated in Fig. 8, after the tertiary PCR reaction, two specific fragments were obtained using the couple of primers TmCAT1-G3/R3 and TmCAT1-G4/R3 and then cloned in pGEM-T EASY vector and ultimately sequenced. The promoter sequence of *TmCAT1* (900 bp) was deposited in GenBank with the accession number MK091460. In order to identify the presence of *cis*-acting regulatory elements, the promoter sequence *PrTmCAT1* was analyzed using PlantCARE database. Several putative *cis*-regulatory elements which are involved in growth and development, hormone signal and abiotic stress responsiveness, were identified in this *PrTmCAT1* sequence. In fact, *PrTmCAT1* sequence contains two *cis*-elements involved in development, viz. the RY-elements and the CCGTCC-box. Besides, this sequence contains three responsive *cis*-acting elements ABRE, four TGACT-motifs involved in MeJA-responsiveness, two GC-motifs involved in anoxic specific inducibility and some of light responsive elements such as GT1-motif and TCT-motif (Fig. 9).

In order to further investigate the regulation mechanisms of catalase genes under environmental conditions, the putative regulatory motifs of *PrTmCAT1* were compared with catalase promoter's genes from bread and durum wheat, barley, *Brachypodium* and rice. Interestingly, *in silico* analysis revealed that the two *cis*-regulatory elements ABRE and TGACT-motifs are present in all these catalase promoter regions. Noticeably, the promoter region of *TmCAT1* contains the highest number of TGACT-motifs (involved in MeJA-responsiveness) and RY-element (involved in seed-specific regulation) (Fig. 9). These results suggest that the presence of all these motifs could play a pivotal role in plant development and modulate the expression of *TmCAT1* under

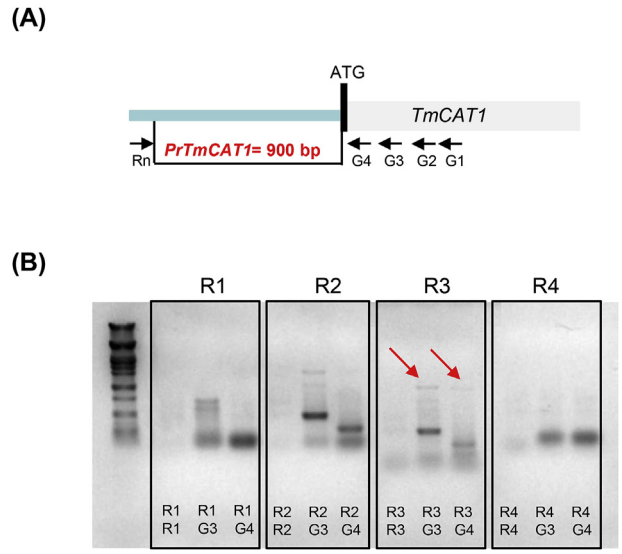

Fig. 8. Isolation of *TmCAT1* promoter sequence by HE-TAIL-PCR method. (A) Schematic representation of the specific primers (G1-G4) allowing chromosome walking in the 5′ direction and random primers (Rn) in the sequence of *TmCAT1* gene (Table1). (B) Analysis of the third TAIL-PCR for promoter sequence of *TmCAT1*. Two target bonds were obtained using TmCAT1-G3/R3 and TmCAT1-G4/R3. The gene specific and random primers used in every reaction are marked at the bottom. M: lambda *Pst*I molecular weight marker.

various stresses.

4. Discussion

In plants, catalase proteins are considered as the most important scavengers of H_2O_2 generated during normal metabolic processes and stress responses (Mhamdi et al., 2012). So far, several *CAT* genes have been identified in both dicotyledonous and monocotyledonous species, and they have been divided into three classes in *Arabidopsis*, tobacco, rice, maize, pumpkin and cucumber plants. In durum wheat, catalase protein TdCAT1, belonging to class I, was isolated and functionally characterized (Feki et al., 2015). In the present study, we isolated the full-length catalase gene *TmCAT1* from the wheat relative *T. monococcum*. The phylogenetic analysis revealed that TmCAT1 is very close to the catalase proteins, belonging to class I from *Triticum*, *Hordeum vulgare*, *Brachypodium distachyon*, *Oryza sativa* and *Arabidopsis thaliana*. Moreover, the analysis of the secondary structure indicated that TmCAT1 presents the calmodulin binding domain and the peroxisomal targeting signal PTS1 motif, similarly to the peroxisomal CAT proteins from other plant species. Concerning the three dimensional structure of CAT1 proteins, the potential structures of TaCAT1 (Sahu et al., 2013) and TdCAT1 (Feki et al., 2015) were predicted, however, no detail pertaining to the oligomerization arrangement of these proteins are available. In this study, we determined, for the first time, the potential 3 and 4D structures of TmCAT1. Accordingly, we used the crystal structure of catalase from *Bacillus pumilus* as a template (Loewen et al., 2015). The analysis revealed that TmCAT1 has a typical three-dimensional conformation with four distinct regions, which are the N-terminal arm (Met1 to Val64), the conserved antiparallel eight-stranded β-barrel (His65 to Ile312), the extended wrapping loop (Asp313 to Asn426), and the C-terminal helical domain (Asn427 to Met492) (Fig. 3A). Based on their physical and biochemical properties, catalases were classified into four types, i.e. monofunctional heme-containing catalases, catalase–peroxidases, non-heme catalases and minor catalases. The most extensively characterized class is the first one, which is present ubiquitously in microorganisms, animals and plants (Sahu et al., 2013; Sooch et al., 2014). As described by Sooch et al. (2014), typical catalases (monofunctional) were formed by four identical subunits and each subunit had one ferric heme prosthetic group (protoporphyrin IX). The heme group, localized between the internal walls of the beta barrel and several helices, is involved in the catalytic activity. The heme group of TmCAT1 catalase is composed of the same residues, forming the heme group of wheat TdCAT1 catalase, i.e. His 65, Ser l04, Asn 138, Arg 344 and Tyr 348 (Feki et al., 2015). The 4D structure of TmCAT1, generated using SymmDock server, evinced an arrangement in asymmetric unit that involves interactions incorporating mainly residues from the N-terminal part (Fig. 3B and C). Similarly, TmCAT1 has a similar oligomerization arrangement with the monofunctional heme catalase protein from *Deinococcus radiodurans* (Borges et al., 2014).

In general, catalases are present essentially in peroxisomes, which play a key role in lipid metabolism, photorespiration, and hormone metabolism, as well as in plant responses to abiotic and biotic stresses (Kaur and Hu, 2011; Hu et al., 2012). It has been reported that the peroxisomal proteins are targeted to the peroxisomes matrix by a conserved peroxisome targeting signal of either type 1 (PTS1) or type 2 (PTS2). The PTS1 motif is more commonly found in plants compared to PTS2, and it is usually used for peroxisome targeting protein prediction (Wang et al., 2017). It comprises about 15 amino acids at the C-terminal ends and it is often largely determined by the PTS1 composed of the QKL tripeptide. Interestingly, TmCAT1, like durum wheat catalase TdCAT1, harbors the QKL tripeptide which is located at −13 to −11 from the C-terminus. In this study, we demonstrated that the PTS1 motif of the two wheat catalases TmCAT1 and TdCAT1 plays a crucial role in their subcellular localization. In fact, the expression of full proteins fused to the GFP in tobacco cells showed a peroxisomal localization. However, the truncated forms TmCAT1Δ_{PTS1} and TdCAT1Δ_{PTS1} remained in the cytosol (Fig. 4B, f and l). Similarly, it has been previously shown that the pumpkin catalase (Cat1) is imported into peroxisomes by the PTS1 system (Kamigaki et al., 2003). The three amino acids (PSI) from the C-terminus of this catalase were shown to be unnecessary for catalase import, whereas the QKL tripeptide was important for targeting catalase into peroxisomes. The analysis using the yeast two-hybrid system demonstrated that pumpkin Cat1 interacts with the peroxisomal biogenesis factors Peroxin 5 (PEX5), allowing the entry of catalase into peroxisomes (Oshima et al., 2008). Recently, Fujikawa et al. (2018) have emphasized the importance of the positions 11 to 4 from the C-terminus of AtCAT2 in catalase import and shed more light on the importance of the amino acid Leu11. It was found that when this amino acid was substituted by glycine, AtCAT2 was not capable of infiltrating into peroxisomes (Fujikawa et al., 2018). It has also been reported that a small heat shock protein Hsp17.6CII can interact with AtCAT2 in the peroxisome and activates its activity (Li et al., 2017). Hsp17.6CII contains the QKL tripeptide upstream from the C-terminus, which is required for its peroxisomal localization and mutations in this tripeptide, leading to the abolishment of this activity.

Catalase genes from different plant species have been shown to play central roles in plant response to both abiotic and biotic stresses (Du et al., 2008; Su et al., 2014; Feki et al., 2015; Alam and Ghosh, 2017). In order to further elucidate the role of *TmCAT1* in *Triticum monococcum*, its expression profile was analyzed in different tissues and under various environmental conditions. Under normal condition, *TmCAT1* is strongly expressed in leaves (Fig. 5). Similarly, the expression of *AtCAT2* in *Arabidopsis* and *OsCATC* in rice are highly detected in leaves (Du et al., 2008; Alam and Ghosh, 2017). The presence of stress strongly enhances the expression of *TmCAT1*. In fact, in response to salt, oxidative, osmotic and heavy metal stresses, the accumulation level of *TmCAT1* transcripts is more considerable in roots compared to leaves, whereas in the presence of hormonal stress, *TmCAT1* is significantly induced in leaves (Fig. 6). It is well known that salicylic acid is considered as a crucial signaling molecule in defense responses. The expression level of *TmCAT1* increases by a factor close to 4 after 3 days of salicylic acid treatment, suggesting that *TmCAT1* could participate as a positive regulator of defense responses in *Triticum monococcum*. In

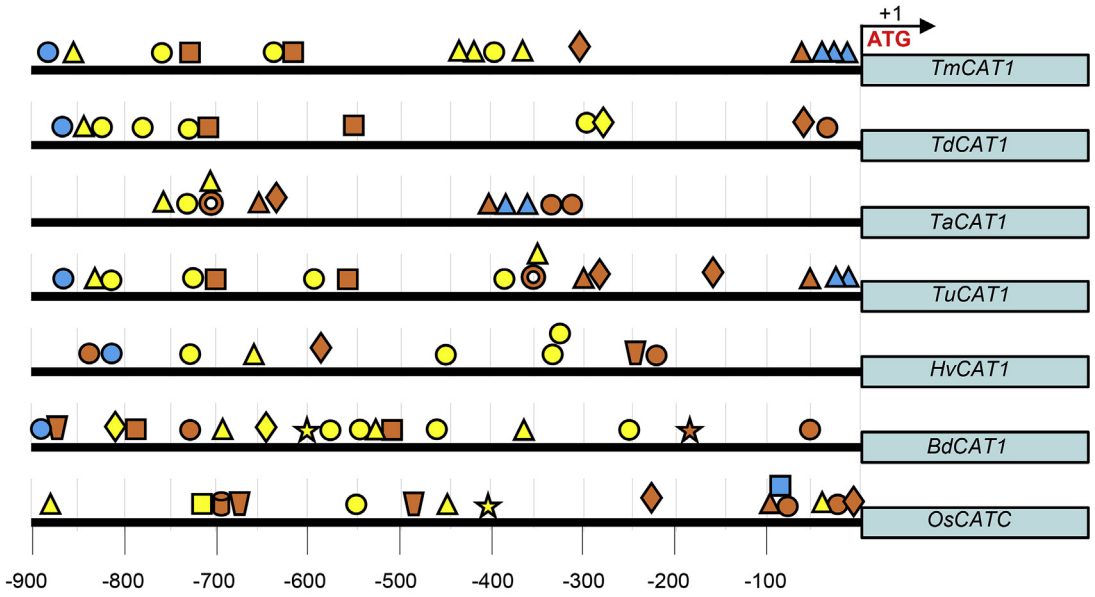

	Sign	Motif	Function	*TmCAT1*	*TdCAT1*	*TaCAT1*	*TuCAT1*	*HvCAT1*	*BdCAT1*	*OsCATC*
Stress	●	ARE	essential for the anaerobic induction	-	1	2	-	2	2	2
	■	GC-motif	involved in anoxic specific inducibility	2	2	-	2	-	2	-
	▲	GT1-motif	light responsive element	1	-	2	2	-	-	1
	♦	TCT-motif	part of a light responsive element	1	1	1	2	1	-	2
	★	TC-rich repeats	involved in defense and stress responsiveness	-	-	-	-	-	1	-
	▼	LTR	involved in low-temperature responsiveness	-	-	-	-	1	1	2
	▮	MBS	MYB binding site involved in drought-inducibility	-	-	-	-	-	-	1
	◎	WUN-motif	Wound-responsive element	-	-	1	1	-	-	-
Hormones	●	ABRE	involved in the abscisic acid responsiveness	3	4	1	4	4	4	1
	■	P-box	gibberellin-responsive element	-	-	-	-	-	-	1
	▲	TGACT-motif	involved in the MeJA-responsiveness	4	1	2	2	1	3	3
	♦	TGA-element	auxin-responsive element	-	1	-	-	-	2	-
	★	TCA-element	involved in salicylic acid responsiveness	-	-	-	-	-	1	1
Development	●	CCGTCC-box	related to meristem specific activation	1	1	-	1	1	1	-
	■	GCN4_motif	involved in endosperm expression	-	-	-	-	-	-	1
	▲	RY-element	involved in seed-specific regulation	3	-	2	2	-	-	-

Fig. 9. Putative *cis*-regulatory elements identified in *PrTmCAT1* and other catalase promoters from wheat, barley, *Brachypodium* and rice. The 900 bp 5′ upstream region from the transcription start site was analyzed bioinformatically using PlantCARE database. The corresponding promoters were retrieved from phytozome and gramene databases. The identifiers are: *Triticum turgidum* TdCAT1 (TGAC_WGS_durum_v1_contig_377865), *Triticum aestivum* TaCAT1 (TRIAE_CS42_5AL_TGACv1_376544_AA1238210), *Triticum urartu* TuCAT1 (TRIUR3_26493), *Hordeum vulgare* HvCAT1 (HORVU4Hr1G082040), *Brachypodium distachyon* BdCAT1 (BRADI1G76330), *Oryza sativa* OsCATC (LOC_Os03g03910). Amount of stress-related (e.g. defense, low temperature, drought, light and wound), hormone-related (e.g. ABA, MeJA, GA, auxin and SA) and developmental-related elements were identified in the catalase promoters. Identified *cis*-acting regulatory elements such as, ARE, GC-motif, GT1-motif, TCT-motif, TC-rich repeats, LTR, MBS, WUN-motif, ABRE, P-box, TGACT-motif TGA-element, CCGTCC-box, GCN4-motif, RY-element, were indicated in the figure with different artworks. The approximate position of the motifs could be identified using the scale provided below.

several studies, it was demonstrated that the expression of catalase genes was induced by environmental conditions in different plants species, such as *Arabidopsis* (Du et al., 2008) and durum wheat (Feki et al., 2015).

Overall, heavy metals such as cadmium, manganese, zinc and copper induce the generation of oxidative stress. Under these

conditions, catalase is considered as the most important enzyme involved in ROS scavenging and, in this respect, there is vigorous evidence that this enzyme confers tolerance to metal stress in plants (Singh et al., 2016; Ben Saad et al., 2018). Interestingly, our results revealed that under cadmium stress, the induction of *TmCAT1* reached a higher level after 72 h of treatment in roots, suggesting the involvement of *TmCAT1* in plant metal response. On the other hand, *TmCAT1* is able to improve stress tolerance of yeast cells under salt, direct oxidative stress, osmotic and heat stresses, except LiCl stress. This finding contrasts with what has previously been reported in the expression of durum wheat *TdCAT1* in yeast cells that tolerate high concentration of lithium in the medium (Feki et al., 2015).

To gain further insight into the regulatory mechanism of *TmCAT1* gene expression, the promoter region of *TmCAT1* was isolated using the thermal asymmetric interlaced PCR (TAIL-PCR) technique (Fig. 8). Although the 5′-flanking regions of catalase genes have been identified and characterized from several plant species such as *Arabidopsis*, rice and maize (Guan et al., 2000; Alam and Ghosh, 2017), little is known about the transcription factors and *cis*-acting regulatory elements that regulate the expression of catalase genes in wheat during stress. The analysis of 900 bp of *TmCAT1* promoter sequence revealed the presence of numerous important *cis*-acting elements, such as the GC-motif, GT1-motif, TCT-motif, ABRE, TGACT-motif, CCGTCC-box and RY-element, suggesting that the expression of *TmCAT1* gene is tightly regulated by environmental conditions (Fig. 9). Compared with catalase promoters from wheat, barley, *Brachypodium* and rice, *TmCAT1* promoter harbored the highest number of TGACT-motifs (involved in MeJA-responsiveness) and RY-elements (involved in seed-specific regulation). However, elements putatively involved in the response to ABA were found in all promoter regions.

5. Conclusion

In conclusion, the isolated catalase from *Triticum monococcum*, TmCAT1 has a peroxisomal localization. The expression level of this gene was up-regulated by various environmental conditions in roots and leaves. In addition, TmCAT1 was able to improve yeast cells growth under various stress conditions. The promoter region of *TmCAT1* analyzed in this study might prove beneficial for the overexpression of *TmCAT1* in transgenic plants and could provide new light on its role and function in wheat.

Author's contribution

ST, KF and FB conceived and designed the experimental plan. ST, YK, CA and HZ performed the experiments and wrote the manuscript. ST, SJ, MNS, CA and FB analyzed the data and revised the manuscript. All the authors agreed on the contents of the paper and post no conflicting interest.

Conflicts of interest

The authors declare that they have no conflict of interest.

Acknowledgements

This study was supported by a grant from the Ministry of Higher Education and Scientific Research, Tunisia. Part of this work was conducted at INRA-SupAgro, Montpellier- France. Thanks are due to the “Plateforme Histocytologie et Imagerie Cellulaire Végétale”, INRA-CIRAD, Montpellier, France.

References

Alam, N.B., Ghosh, A., 2017. Comprehensive analysis and transcript profiling of *Arabidopsis thaliana* and *Oryza sativa* catalase gene family suggests their specific roles in development and stress responses. Plant Physiol. Biochem. 123, 54–64.

Ben Saad, R., Hsouna, A.B., Saibi, W., Hamed, K.B., Brini, F., Ghneim-Herrera, T., 2018. A stress-associated protein, LmSAP, from the halophyte Lobularia maritima provides tolerance to heavy metals in tobacco through increased ROS scavenging and metal detoxification processes. J. Plant Physiol. 231, 234–243.

Borges, P.T., Frazão, C., Miranda, C.S., Carrondo, M.A., Romão, C.V., 2014. Structure of the monofunctional heme catalase DR1998 from Deinococcus radiodurans. FEBS J. 281, 4138–4150.

Caffrey, D.R., Somaroo, S., Hughes, J.D., Mintseris, J., Huang, E.S., 2004. Are protein-protein interfaces more conserved in sequence than the rest of the protein surface? Protein Sci. 13, 190–202.

Chen, H.J., Wu, S.D., Huang, G.J., Shen, C.Y., Afiyantia, M., Li, W.J., Lin, Y.H., 2012. Expression of a cloned sweet potato catalase SPCAT1 alleviates ethephon-mediated leaf senescence and H_2O_2 elevation. J. Plant Physiol. 169, 86–97.

Choudhury, F.K., Rivero, R.M., Blumwald, E., Mittler, R., 2016. Reactive oxygen species, abiotic stress and stress combination. Plant J. 90, 856–867.

Choudhury, S., Panda, P., Sahoo, L., Panda, S.K., 2013. Reactive oxygen species signaling in plants under abiotic stress. Plant Signal. Behav. 8, 23681.

Das, P., Nutan, K.K., Singla-Pareek, Sneh, L., Pareek, A., 2015. Oxidative environment and redox homeostasis in plants: dissecting out significant contribution of major cellular organelles. Front Environ Sci 2, 70.

Davenport, R., James, R.A., Zakrisson-Plogander, A., Tester, M., Munns, R., 2005. Control of sodium transport in durum wheat. Plant Physiol. 137, 807–818.

Du, Y.Y., Wang, P.C., Chen, J., Song, C.P., 2008. Comprehensive functional analysis of the catalase gene family in Arabidopsis thaliana. J. Integr. Plant Biol. 50, 1318–1326.

Feki, K., Kamoun, Y., Mahmoud, R.B., Farhat-Khemakhem, A., Gargouri, A., Brini, F., 2015. Multiple abiotic stress tolerance of the transformants yeast cells and the transgenic Arabidopsis plants expressing a novel durum wheat catalase. Plant Physiol. Biochem. 97, 420–431.

Frugoli, J.A., Zhong, H.H., Nuccio, M.L., McCourt, P., McPeek, M.A., Thomas, T.L., McClung, C.R., 1996. Catalase is encoded by a multigene family in Arabidopsis thaliana (L.) Heynh. Plant Physiol. 112, 327–336.

Fujikawa, Y., Suekawa, M., Endo, S., Fukami, Y., Mano, S., Nishimura, M., Esaka, M., 2018. Effect of mutation of C-terminal and heme binding region of Arabidopsis catalase on the import to peroxisomes. Biosci. Biotechnol. Biochem. 8, 1–4.

Garcia, R., Kaid, N., Vignaud, C., Nicolas, J., 2000. Purification and some properties of catalase from wheat germ (Triticum aestivum L.). J. Agric. Food Chem. 48, 1050–1057.

Gietz, R.D., Schiestl, R.H., Willems, A.R., Woods, R.A., 1995. Studies on the transformation of intact yeast cells by the LiAc/SS-DNA/PEG procedure. Yeast 11, 355–360.

Giri, M.K., Singh, N., Banday, Z.Z., Singh, V., Ram, H., Singh, D., Chattopadhyay, S., Nandi, A.K., 2017. GBF1 differentially regulates *CAT2* and *PAD4* transcription to promote pathogen defense in *Arabidopsisthaliana*. Plant J. 91, 802–815.

Guan, L., Scandalios, J.G., 1995. Developmentally related responses of maize catalase genes to salicylic acid. Publ. Nat. Sci. 92, 5930–5934.

Guan, L.M., Zhao, J., Scandalios, J.G., 2000. Cis-elements and trans-factors that regulate expression of the maize Cat1 antioxidant gene in response to ABA and osmotic stress: H_2O_2 is the likely intermediary signaling molecule for the response. Plant J. 22, 87–95.

He, H., Van Breusegem, F., Mhamdi, A., 2018. Redox-dependent control of nuclear transcription in plants. J. Exp. Bot. 69, 3359–3372.

Hu, J., Baker, A., Bonnie, B., Linka, N., Mullen, R.T., Reumann, S., Zolman, B.K., 2012. Plant peroxisomes: biogenesis and function. Plant Cell 24, 2279–2303.

Iwamoto, M., Higo, H., Higo, K., 2000. Differential diurnal expression of rice catalase genes: the 5′- flanking region of CatA is not sufficient for circadian control. Plant Sci. 151, 39–46.

Kamigaki, A., Mano, S., Terauchi, K., Nishi, Y., Tachibe-Kinoshita, Y., Nito, K., Kondo, M., Hayashi, M., Nishimura, M., Esaka, M., 2003. Identification of peroxisomal targeting signal of pumpkin catalase and the binding analysis with PTS1 receptor. Plant J. 33, 161–175.

Kaur, N., Hu, J., 2011. Defining the plant peroxisomal proteome: from A*rabidopsis* to rice. Front. Plant Sci. 2, 1–41.

Li, G., Li, J., Hao, R., Guo, Y., 2017. Activation of catalase activity by a peroxisome-localized small heat shock protein Hsp17.6CII. J Genet Genomics 44, 395–404.

Livak, K.J., Schmittgen, T.D., 2001. Analysis of relative gene expression data using real-time quantitative PCR and the 2_DDCT method. Methods 25, 402–408.

Loewen, P.C., Villanueva, J., Switala, J., Donald, L.J., Ivancich, A., 2015. Structure of *Bacillus pumilus* catalase. Proteins 83, 853–866.

Matsumura, T., Tabayashi, N., Kamagataa, Y., Soumaa, C., Saruyama, H., 2002. Wheat catalase expressed in transgenic rice can improve tolerance against low temperature stress. Physiol. Plantarum 116, 317–327.

Mhamdi, A., Noctor, G., Baker, A., 2012. Plant catalases: peroxisomal redox guardians. Arch. Biochem. Biophys. 525, 181–194.

Mhamdi, A., Queval, G., Chaouch, S., Vanderauwera, S., Van Breusegem, F., Noctor, G., 2010. Catalase function in plants: a focus on Arabidopsis mutants asstress-mimic models. J. Exp. Bot. 61, 4197–4220.

Michiels, A., Tucker, M., Van den Ende, W., Van Laere, A., 2003. Chromosomal walking of flanking regions from short known sequences in GC-rich plant genomic DNA. Plant Mol. Biol. Rep. 21, 295–302.

Miller, G., Suzuki, N., Ciftci-Yilmaz, S., Mittler, R., 2010. Reactive oxygen species homeostasis and signalling during drought and salinity stresses. Plant Cell Environ. 33, 453–467.

Mittler, R., 2002. Oxidative stress, antioxidants and stress tolerance. Trends Plant Sci. 7, 405–410.

Nelson, B.K., Cai, X., Nebenführ, A., 2007. A multicolored set of *in vivo* organelle markers for co-localization studies in *Arabidopsis* and other plants. Plant J. 51, 1126–1136.

Noctor, G., Foyer, C.H., 2016. Intracellular redox compartmentation and ROS-related communication in regulation and signaling. Plant Physiol. 171, 1581–1592.
Oshima, Y., Kamigaki, A., Nakamori, C., Mano, S., Hayashi, M., Nishimura, M., Esaka, M., 2008. Plant catalase is imported into peroxisomes by Pex5p but is distinct from typical PTS1 import. Plant Cell Physiol. 49, 671–677.
Piovesan, D., Minervini, G., Tosatto, S.C., 2016. The RING 2.0 web server for high quality residue interaction networks. Nucleic Acids Res. 8, 367–374.
Sahu, G.K., Sahoo, B.B., Bhandari, S., Pandey, S., 2013. In silico 3D structure prediction and hydrogen peroxide binding study of wheat catalase. Interdiscip Sci 5, 77–83.
Scandalios, J.G., 2005. Oxidative stress: molecular perception and transduction of signals triggering antioxidant gene defenses. Braz J Med Res 38, 995–1014.
Schneidman-Duhovny, D., Inbar, Y., Nussinov, R., Wolfson, H.J., 2005. Geometry based flexible and symmetric protein docking. Proteins 60, 224–231.
Singh, S., Parihar, P., Singh, R., Singh, V.P., Prasad, S.M., 2016. Heavy metal tolerance in plants: role of transcriptomics, proteomics, metabolomics, and ionomics. Front. Plant Sci. 6, 1143.
Skadsen, R.W., Schulze-Lefert, P., Herbst, J.M., 1995. Molecular cloning, characterization and expression analysis of two catalase isozyme genes in barley. Plant Mol. Biol. 29, 1005–1014.
Sooch, B.S., Kauldhar, B.S., Puri, M., 2014. Recent insights into microbial catalases: isolation, production and purification. Biotechnol. Adv. 32, 1429–1447.
Sparkes, I.A., Runions, J., Kearns, A., Hawes, C., 2006. Rapid, transient expression of fluorescent fusion proteins in tobacco plants and generation of stably transformed plants. Nat. Protoc. 1 (4), 2019–2025 2006.
Su, T., Wang, P., Li, H., Zhao, Y., Lu, Y., Dai, P., Ren, T., Wang, X., Li, X., Shao1, Q., Zhao, D., Zhao, Y., Ma, C., 2018. The *Arabidopsis* catalase triple mutant reveals important roles of catalases and peroxisome derived signaling in plant development. J. Integr. Plant Biol. 60, 591–607.
Su, Y., Guo, J., Ling, H., Chen, S., Wang, S., Xu, L., Allan, A.C., Que, Y., 2014. Isolation of a novel peroxisomal catalase gene from sugarcane, which is responsive to biotic and abiotic stresses. PLoS One 9, 84426.
Wang, J., Wang, Y., Gao, C., Jiang, L., Guo, D., 2017. PPero, a computational model for plant PTS1 Type peroxisomal protein prediction. PLoS One 12, 0168912.
Weigel, D., Glazebrook, J., 2006. Transformation of agrobacterium using the freeze-thaw method. CSH Protoc. 2006 (7). https://doi.org/10.1101/pdb.prot4668. pii: pdb.prot4666.
Yang, T., Poovaiah, B.W., 2002. Hydrogen peroxide homeostasis: activation of plant catalase by calcium/calmodulin. Proc. Natl. Acad. Sci. Unit. States Am. 99, 4097–4102.
Zimmermann, P., Heinlein, C., Orendi, G., Zentgraf, U., 2006. Senescence-specific regulation of catalases in *Arabidopsis thaliana* (L.) Heynh. Plant Cell Environ. 29, 1049–1060.